JOURNAL OF MAGNETIC RESONANCE **124,** 80–86 (1997)
ARTICLE NO. MN961015

Lineshapes of Optically Detected Nuclear Magnetic Resonance in GaAs/AlGaAs Heterostructures

M. SCHREINER,* H. HÖCHSTETTER,* H. PASCHER,* AND S. A. STUDENIKIN†

**Experimentalphysik I, Universität Bayreuth, D-95440 Bayreuth, Germany; and †Institute of Semiconductor Physics, 630090 Nowosibirsk, Russia*

Received July 3, 1996; revised September 23, 1996

In different GaAs/AlGaAs heterostructures, nuclear magnetic resonance is detected via a change in the degree of circular polarization of the photoluminescence under excitation with circularly polarized light. Depending on the doping of the sample, the strength of the external magnetic field, the power of the radiofrequency field, and the total time for passing the resonance, different lineshapes are observed. These are understood in terms of the model of a "nuclear Hanle effect" regarding slow- and fast-passage conditions.

INTRODUCTION

The optical detection of nuclear magnetic resonances (ODNMR) in semiconductors provides a very sensitive method compared to conventional NMR. The reason is the high energy of the detected light quanta compared to radiofrequency (*1*). Thus it is possible to use the ODNMR in structured semiconductors as heterostructures, quantum wells (QW), and so on, where only a small number of spins is in the layer of interest. A further advantage of the optical detection is the selectivity, allowing one to distinguish between different layers in a structured sample (*2*). Since the method relies on the excitation of electrons, typically by laser, lateral resolution is also possible by scanning the laser focus across the sample surface.

A successful application of the method requires a detailed understanding of resonance line positions and lineshapes. In this paper we will show and discuss different lineshapes obtained with ODNMR measurements on GaAs/AlGaAs heterostructures arising due to variation of the following parameters: laser intensity, radiofrequency power, resonant magnetic field, and sweep direction.

PRINCIPLES

GaAs has a direct band gap at the Γ point of the Brillouin zone. The valence band consists of heavy hole (hh, $m = \frac{3}{2}$) and light hole (lh, $m = \frac{1}{2}$) states which are degenerate at $k = 0$. This degeneracy is lifted in heterostructures. The split-off valence band is separated by about 0.34 eV from the lh-, hh-valence band.

Exciting the semiconductor with a laser at an energy slightly above the fundamental gap generates electrons in the conduction band (cb), which recombine after a lifetime τ emitting a photoluminescence (PL) photon. The spectral position where the ODNMR is detected selects different sites (e.g., nuclei in certain layers in QWs or quantum dots).

Using circularly polarized light for the excitation results in a spin polarization of the electrons excited into the conduction band. This effect is called optical pumping. The initial electronic polarization will decay with a spin relaxation time τ_s. The detected photoluminescence shows a polarization depending on the actual degree of electronic polarization (*3*).

Due to their s-like wavefunctions, the electrons in the conduction band have a nonzero probability of being at the nuclear sites. This fact gives rise to a nonzero hyperfine interaction. The polarization of the electron-spin system is transferred to the nuclear-spin system via flip-flop processes, thus creating a nuclear-spin polarization significantly above thermal equilibrium. This mechanism is called dynamic nuclear polarization (*4, 5*). Also due to hyperfine interaction, the nuclei act on the electronic-spin system, an interaction which can be described by an effective nuclear field B_n.

The principle of ODNMR may be explained using the model of a nuclear Hanle effect (*6*). In general the Hanle effect (*7*) arises from a magnetic field perpendicular to the wavevector **k** of the exciting light, which defines the direction of electronic polarization. It is easy to show that the electronic-spin polarization and thus the photoluminescence polarization as a function of a transverse magnetic field B is described by a Lorentzian (*8*):

$$P = \frac{P_0}{1 + (B/\Delta B)^2}. \qquad [1]$$

The halfwidth of this curve is

$$\Delta B = \frac{\hbar}{|g^*|\mu_B T_S} \qquad [2]$$

1090-7807/97 $25.00

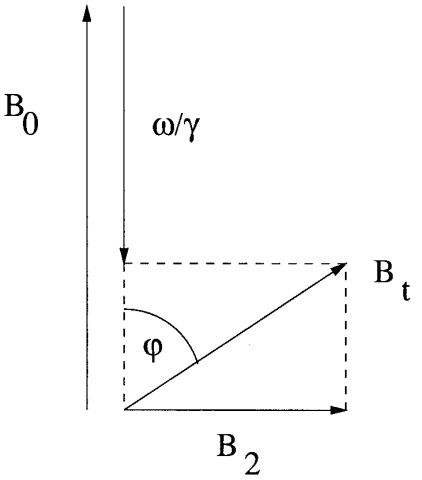

FIG. 1. Alignment of different magnetic fields in the rotating frame. B_0, external field; B_2, radiofrequency field; B_t, effective field; φ, angle between B_0 and B_t.

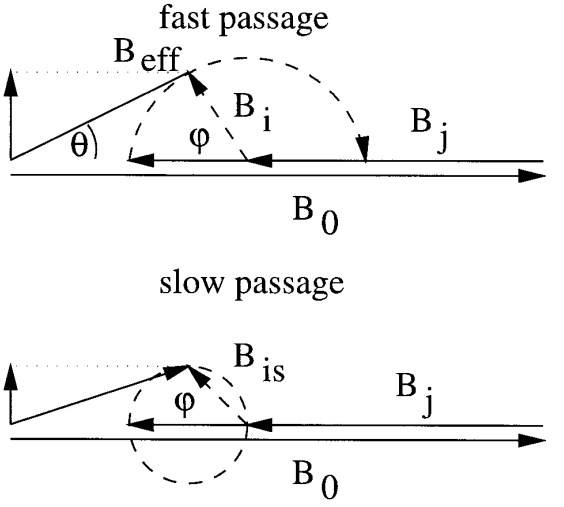

FIG. 2. Slow and adiabatic fast passage in the geometric model; antiparallel geometry. B_0, external magnetic field; B_j, effective field of all nuclei except the species on resonance; B_i, B_{is} field due to species on resonance, aligned $\|$ to B_t (see text). For definition of φ see Fig. 1.

with

$$\frac{1}{T_S} = \frac{1}{\tau} + \frac{1}{\tau_s}. \qquad [3]$$

The effective g factor of the electrons in the conduction band is g^*. By the way, the Hanle effect is a simple method for determining τ and τ_s if g^* is given (*9*). If, however, the angle Θ between the magnetic field $\mathbf{B}$ and $\mathbf{k}$, $\mathbf{S}_z$ is not $\pi/2$ (oblique Hanle effect), then a more complex formula must be used in order to describe the mean electronic polarization (*10*):

$$\langle S_z\rangle(B) = \langle S_z\rangle(B=0)\left[\frac{\sin^2\Theta}{1+(B/\Delta B)^2} + \cos^2\Theta\right]. \qquad [4]$$

This geometry arises during the passage of the NMR.

As in conventional NMR, in ODNMR the radiofrequency magnetic field $\mathbf{B}_2$ is applied perpendicular to the external magnetic field $\mathbf{B}_0$. Introducing the rotating-frame theory with the resonance at an angular frequency $\boldsymbol{\omega}_0 = -\gamma\mathbf{B}_0$, γ being the gyromagnetic ratio, we get for $\mathbf{B}_2$ rotating in the laboratory frame with $\boldsymbol{\omega}$ (*11*)

$$\mathbf{B}_t = \mathbf{B}_0 + \frac{\boldsymbol{\omega}}{\gamma} + \mathbf{B}_2. \qquad [5]$$

Figure 1 shows this arrangement for the slightly off-resonance case. On passing through resonance, $\mathbf{B}_t$ turns by 180° and is aligned with $\mathbf{B}_2$ exactly at resonance.

If the rate at which $\mathbf{B}_t$ tips is slow enough, the magnetization is continuously aligned with $\mathbf{B}_t$. This is true as long as the magnetic field sweep conforms to the condition known as adiabatic fast passage (*12*):

$$\frac{1}{T_1} \ll \frac{1}{B_2}\left|\frac{dB_0}{dt}\right| \ll \gamma B_2. \qquad [6]$$

[In solids T_2 is replaced by T_1 (*13*).] T_1 is of the order of a minute; B_2 depends on the RF power, and we reached values of approximately 0.5 mT.

The mechanism of ODNMR is readily explained by means of a geometric model. The underlying experimental situation is thus: the external magnetic field $\mathbf{B}_0$ is aligned parallel to the direction $\mathbf{k}$ of the propagation of light. Depending on the sign of circular polarization, the nuclei are dynamically polarized either parallel or antiparallel to $\mathbf{B}_0$. The upper part of Fig. 2 shows the principle for adiabatic fast passage, where the nuclei of species i are on resonance. We assume antiparallel geometry, which in experiments yields higher signals. The nuclear magnetic field B_i rotates parallel to $\mathbf{B}_t$ and an effective field $\mathbf{B}_{\text{eff}}$ at an angle Θ provides for the oblique Hanle effect. The electronic polariza-

TABLE 1
Results of Hanle Measurements on the QW Sample, Taken at 820.8 nm

FWHH	[mT]	6.2
τ_s	[ns]	20.9
τ	[ns]	44.2

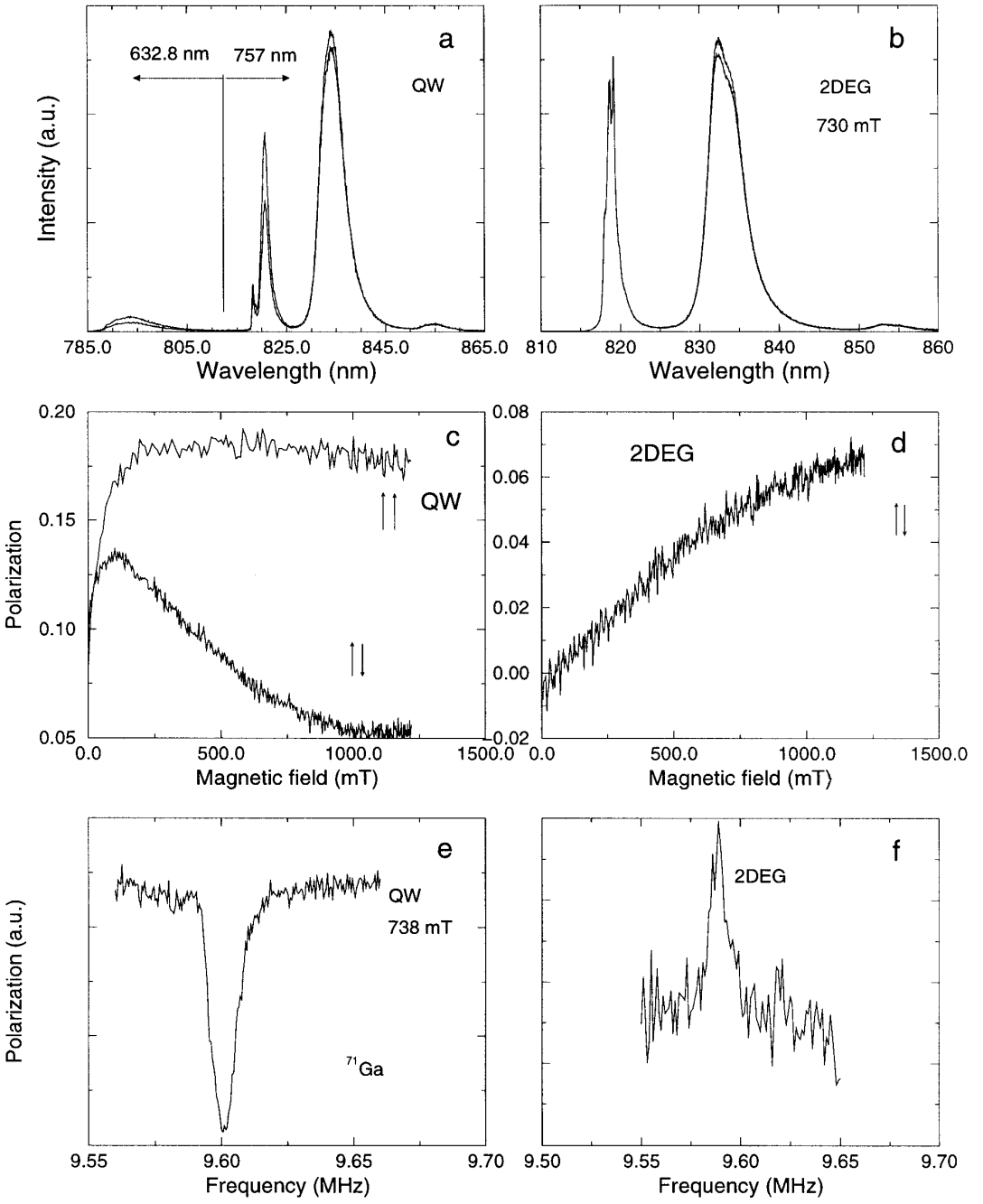

FIG. 3. (a, b) PL spectra of QW and 2-DEG sample. (c, d) Degree of PL polarization vs magnetic field. Trace marked by ⇈, nuclear field parallel to external magnetic field; ⇅, antiparallel. Sample in (d) shows no difference between ⇈ and ⇅. (e, f) Typical recordings of ^{71}Ga ODNMR: degree of polarization vs frequency of radio field at fixed magnetic field.

tion is diminished, reaching a minimum at $\omega = \omega_0$ when Θ is at a maximum.

Passing the resonance with a time constant similar to or slower than the nuclear-spin relaxation time is called slow passage (*14*, *15*). The vector $\mathbf{B}_t$ in the rotating frame now rotates slowly enough that the nuclear field $\mathbf{B}_i$ precesses around $\mathbf{B}_t$. The mean nuclear component exhibits the same direction as in fast passage, but its absolute value is given by the projection B_{is} of $\mathbf{B}_i$ on $\mathbf{B}_t$, leading to a zero value for $\omega = \omega_0$. Consequently exactly on resonance, no Hanle effective transverse component of the nuclear field will exist, and the polarization achieves the same value as far from resonance. Since the nuclear polarization is dynamically rebuilt, a transverse component arises after passing the reso-

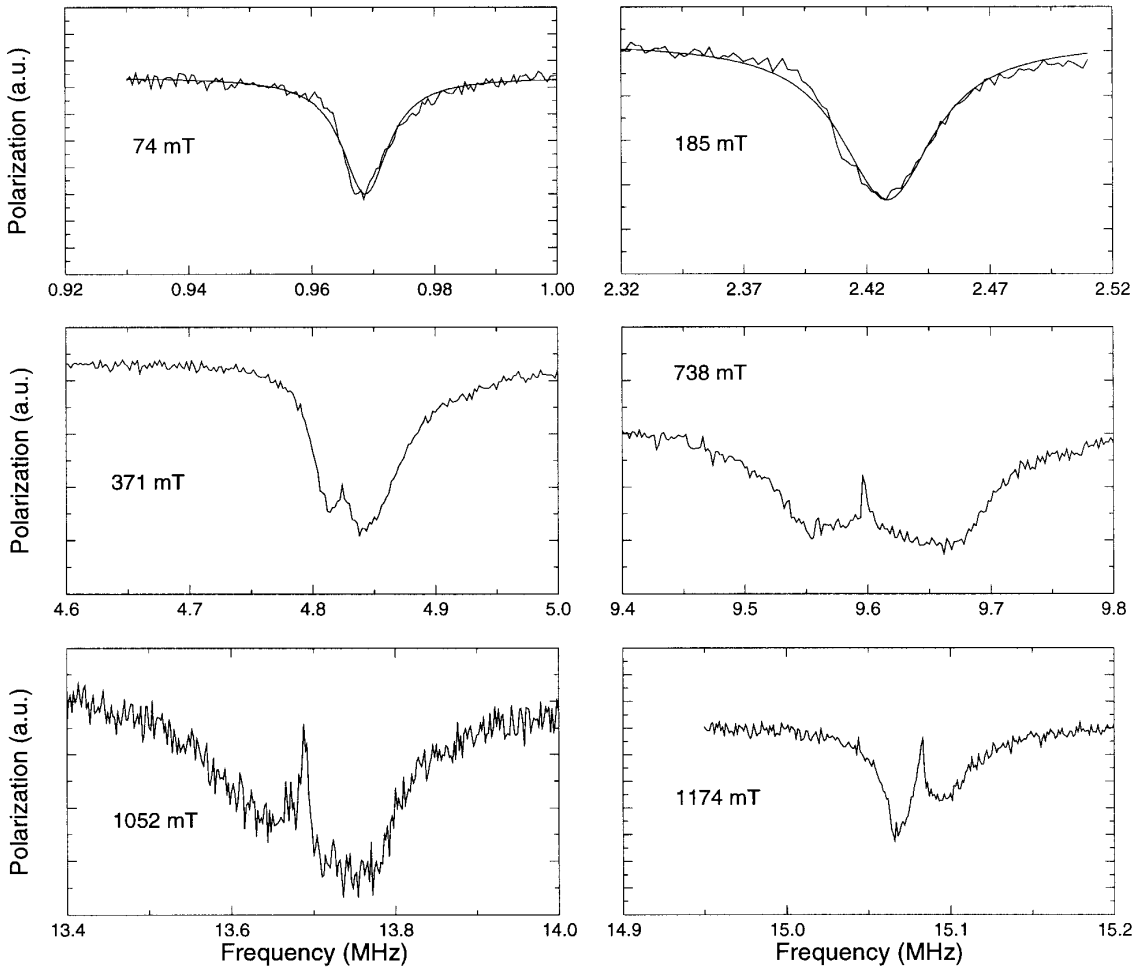

FIG. 4. Typical ^{71}Ga ODNMR lineshapes (degree of PL polarization vs radiofrequency) at various magnetic fields. Further parameters: RF power −18 dB, light intensity 0.3 mW, RF sweep rate 0.6 kHz/s.

nance at ω_0. The experiment shows a typical W shape for the resonance curve (*16*).

EXPERIMENTAL RESULTS AND DISCUSSION

In the ODNMR experiments, the sample was held at $T \approx 1.8$ K in liquid helium in a cryostat bath in the field of an electromagnet. The excitation was done with a diode laser at 757 nm; the circular polarization is adjusted with an electrooptic modulator at constant voltage. The laser is focused onto the sample and the photoluminescence is detected through a 64 cm monochromator by a GaAs photomultiplier. The PL polarization is analyzed in front of the monochromator with a σ^+/σ^- modulator synchronized to a gated photon counter. The degree of polarization $\rho = (I_+ - I_-)/(I_+ + I_-)$ can be calculated instantly. For Hanle measurements, the electrooptic modulator was used with a frequency of 1 kHz for generation of σ^+/σ^- modulated circularly polarized excitation, because no nuclear magnetic field effects were desired. The RF field is generated by a computer-controlled synthesizer, amplified to a maximum of 10 W and irradiated on the sample by a small coil.

A considerable number of different samples has been investigated; two are discussed as examples in the present paper: an undoped GaAs/$Al_{0.8}Ga_{0.2}$As QW structure with a well width of 7.5 nm and a GaAs/AlGaAs heterostructure with a 2-DEG at the GaAs/AlGaAs interface. The QW structure allowed the largest variation of experimental parameters retaining a good signal-to-noise ratio; the n-type heterostructure is remarkable since the experiment is based on spin pumping, which usually only works with p-type material.

Hanle measurements at the spectral position where NMR was performed were taken for the QW sample. The results are presented in Table 1. Figures 3a and 3b show luminescence spectra of the QW and 2-DEG sample. The two traces are for the two circular polarizations. The bands around 835 nm are due to carbon acceptors, and around 820 nm is the excitonic emission. In the QW sample an additional peak

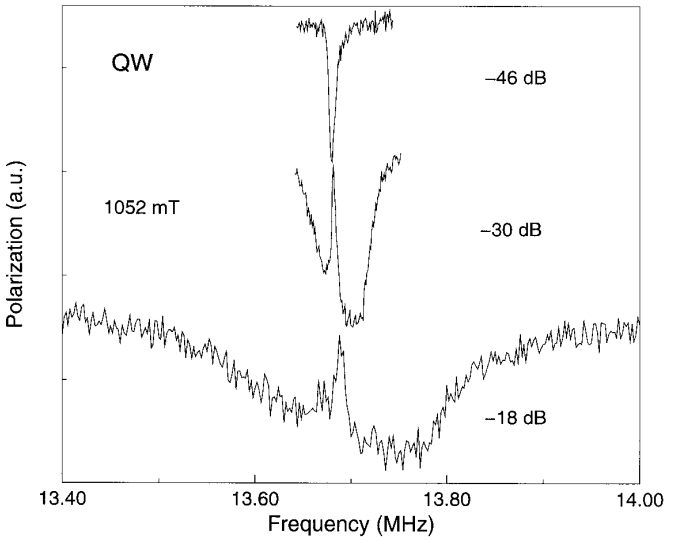

FIG. 5. ^{71}Ga ODNMR lineshapes at different power levels of the radio-frequency field. Further parameters: light intensity 0.3 mW, RF sweep rate 0.6 kHz/s.

shifted to higher energies due to confinement is observed if an excitation wavelength of 632.8 nm is used; usually the excitation was at 757 nm. The PL band at 790 nm of the QW sample reveals no NMR signal, most probably due to improper relaxation times. All NMR experiments shown in the present paper with this sample were done at 820.8 nm, where, due to the higher degree of polarization, the signal-to-noise ratio is far better than in the C-acceptor band. The PL spectrum of the 2-DEG sample exhibits polarization only when a magnetic field is applied, and even at 730 mT only a few percent is reached at the broad C-acceptor line.

The PL polarization in dependence on the magnetic field is shown in Figs. 3c and 3d. For the QW the cases for parallel and antiparallel geometry are drawn. The latter geometry results in a decrease of polarization for higher fields, which is due to the nuclear magnetic field which cancels the external field. For parallel geometry the nuclear field enlarges the external field and a higher polarization is achieved. The polarization of the 2-DEG sample reveals a steadily growing behavior, starting at zero for $B = 0$ mT. Figures 3e and 3f give examples for NMR measurements revealing the most interesting difference between these two samples, which is the decrease of polarization on resonance for the QW sample as is expected from the previous discussion of the nuclear Hanle effect. For the 2-DEG sample, however, an increase in the degree of polarization is observed on resonance.

As described under Principles, we usually expect a decrease in the degree of polarization due to a component of the magnetic field perpendicular to **k**. This is exactly what we see in Fig. 3e. For an explanation of the unexpected behavior found in the 2-DEG sample, one must keep in mind that optical pumping of an n-doped sample is not as effective as in p-type or intrinsic material. As a consequence, the PL sample is unpolarized at $B = 0$. Polarization is induced by a magnetic field (see Fig. 3d). Before passing the resonance, we have a total magnetic field $\mathbf{B}_{\text{eff}} = \mathbf{B}_0 - \Sigma_k \mathbf{B}_k$, where $\mathbf{B}_k$ are the ''nuclear magnetic fields'' of the relevant nuclei (^{75}As, ^{69}Ga, and ^{71}Ga). The ''minus'' is due to antiparallel geometry. On resonance, $\mathbf{B}_i$ is turned 90° from the B_0 direction (z) and the component in the z direction of $\mathbf{B}_{\text{eff}}$ is enhanced. Taking into account the $P(B)$ plot in Fig. 3d, the observed increase in polarization is understood. This argument holds as long as the nuclear field B_i is relatively small and no significant Hanle-effect transverse component is active. The fact that the nuclear fields are smaller than in the QW sample may be deduced from the fact that there is no cancellation effect (decrease of polarization at higher B) in the $P(B)$ spectrum even in antiparallel geometry (see Fig. 3d).

In Fig. 4 resonance lineshapes of the ^{71}Ga nucleus at different values of the external magnetic field are shown. For comparison of the linewidths note that the frequency span is different. With increasing field a broadening of the resonance line occurs, and, at higher magnetic fields (>371 mT), a sharp peak in the center evolves which for the higher-field cases above 1 T almost reaches the off-resonance polarization. In contrast to the other panels, the sweep in the lower right panel of Fig. 4 was performed from low to high frequency which causes a typical change in the asymmetry.

Figure 5 demonstrates the dependence of the linewidth and lineshape on RF power, for the ^{71}Ga nucleus at an external magnetic field of 1052 mT. In Fig. 4 at this field the line is already W shaped, but reducing the RF power results in a dramatic decrease in the linewidth and one obtains a sharp, almost symmetric resonance line.

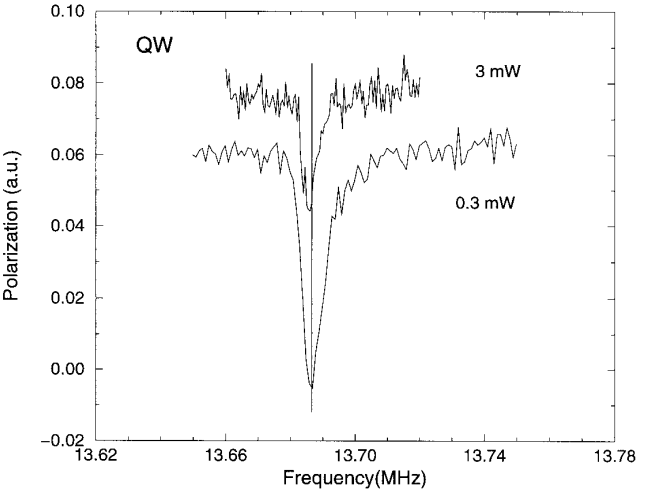

FIG. 6. ^{71}Ga ODNMR lineshapes at two different power levels of the exciting laser. Further parameters: RF power −45 dB, RF sweep rate 0.6 kHz/s, B_0 1052 mT.

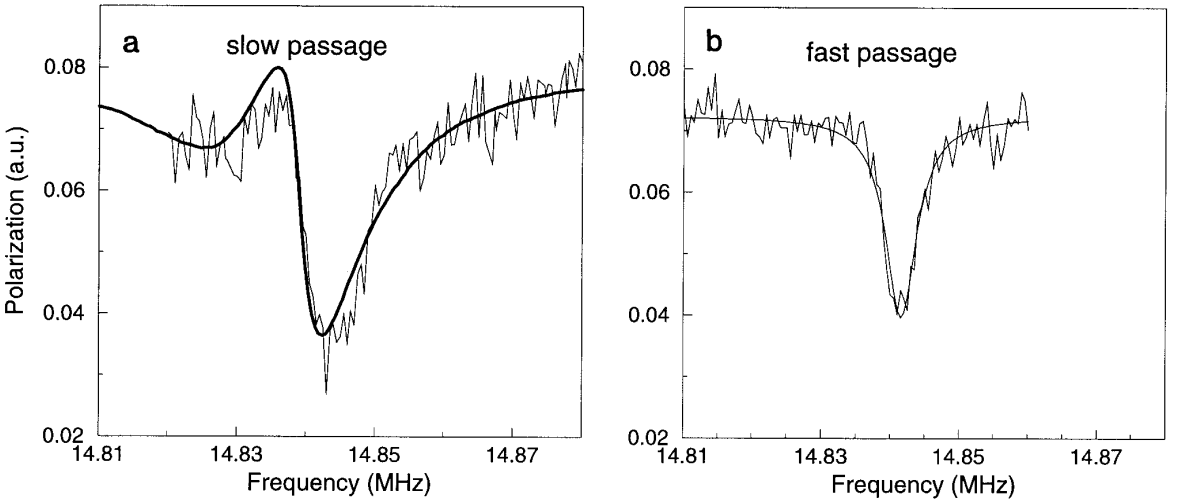

FIG. 7. ^{71}Ga ODNMR lineshapes at two different radiofrequency sweep rates (slow, 0.2 kHz/s; fast, 2.0 kHz/s); solid line in slow passage, lineshape calculated by computer simulation. Experimental parameters: RF power −40 dB, B_0 1140 mT, light intensity 0.3 mW.

Figure 6 compares two NMR signals taken with 0.3 and 3 mW laser intensity, respectively. The reduction of the degree of polarization on resonance is diminished but the lineshape does not change despite a small Knight shift due to the electronic polarization increased by higher laser power. There is obviously no evidence for line broadening or W shaping.

In Fig. 7 two different speeds for the sweep of the RF frequency were used to measure the NMR. The curve in Fig. 7b was taken under fast-passage conditions, and Fig. 7a shows the transition to slow passage, exhibiting an asymmetry and a W shape.

As shown in Figs. 4, 5, and 7, under different conditions structured lineshapes of NMR resonances are obtained. The mechanism, however, which leads to the W shape is always the same. It is clear that the speed of the sweep across the resonance determines whether fast- or slow-passage conditions are fulfilled, but dependence on external field and RF power can be explained in the same context.

The applied RF power directly determines the amplitude of the rotating field B_2 (Fig. 1). It is clear that, passing through resonance with higher B_2, the angle φ between B_0 and B_t reaches the same value at an ω farther away from resonance than in the case with smaller B_2. Thus the pass through resonance starts at a larger distance from resonance and the line broadens. Keeping the same speed of the frequency sweep, the passing time elongates, causing the system to leave the fast-passage regime and to perform a slow passage, where the W shape is obtained.

For an explanation of the dependence of the NMR lineshape on the external field, Fig. 2 is applicable. Due to the fact that the nuclear magnetic field is increasing nonlinearly with the external field (*10*), the same tip angle φ (of B_t) leads to an enhanced angle θ of the Hanle-effect component. Thereby the resonance curve broadens as well, and, since the frequency sweep rate is constant, the resonance passage is changed from fast to slow and the peak at ω_0 appears.

The lineshape models can be checked with a simulation using a Monte Carlo method for the nuclear polarization. For each time step, dynamic polarization as well as nuclear-spin relaxation is taken into account by orienting nuclei on a two-dimensional lattice. The influence of the RF field is considered in the geometric model according to Figs. 1 and 2. Finally the PL polarization is calculated according to Eq. [4].

It should be pointed out that this simulation refers to both fast- and slow-passage conditions and thus also correctly describes intermediate situations. All nuclei are rotating with B_t. Depending on the relation of nuclear relaxation time to sweep rate, the projection of the nuclear magnetization on B_t is larger or smaller (fast or slow passage). By varying parameters like RF power, RF sweep rate, and nuclear relaxation time, one can obtain lineshapes as observed experimentally. For fast-passage conditions, an asymmetric shape is yielded, which changes to the W shape for slower passages. The solid line without noise in Fig. 7a is the result of such a simulation performed with parameters according to the experimental conditions. This simulation then allows the determination of the nuclear-spin relaxation time which is 2.5 min for ^{71}Ga in the sample demonstrated in Fig. 7.

CONCLUSIONS

The geometric model for the optical detection of NMR allows description of the various lineshapes observed in such an experiment. An increase in the degree of PL polarization in n-doped material as well as the occurrence of W-shaped lines is well described by the nuclear Hanle effect within the geometric model.

ACKNOWLEDGMENTS

Financial support from the Emil-Warburg-Foundation and DFG (Graduiertenkolleg) is gratefully acknowledged. We thank A. I. Toropov for growing the samples.

Note added in proof. Another possible explanation for a lineshape as observed in Fig. 3f is that only the central peak of an extremely broad W-shaped line is detected.

REFERENCES

1. D. Suter, *J. Magn. Reson.* **90,** 495 (1992).
2. G. P. Flinn, R. T. Harley, M. J. Snelling, A. C. Tropper, and T. M. Kerr, *J. Luminesc.* **45,** 218 (1990).
3. B. C. Cavenett, *Adv. Phys.* **30**(4), 475 (1981).
4. A. Abragam, ''The Principles of Nuclear Magnetism,'' Chap. 6, Clarendon Press, Oxford, 1961.
5. D. Paget, *Phys. Rev. B* **25**(7), 4444 (1982).
6. D. Paget, G. Lampel, B. Sapoval, and V. I. Safarov, *Phys. Rev. B* **15,** 5780 (1977).
7. W. Hanle, *Z. Phys.* **30,** 93 (1924).
8. M. I. Dyakonov and V. I. Perel, ''Optical Orientation'' (F. Meier and B. P. Zakharchenya, Eds.), Chap. 2, North-Holland, Amsterdam, 1984.
9. M. Schreiner, M. Krapf, H. Pascher, G. Denninger, G. Weimann, and W. Schlapp, *Superlatices Microstruct.* **11**(4), 409 (1992).
10. M. I. Dyakonov, V. I. Perel, V. L. Berkovits, and V. I. Safarov, *Sov. Phys.-JETP* **40,** 950 (1975).
11. T. C. Farrar and E. D. Becker, ''Pulse and Fourier Transform NMR,'' Academic Press, New York, 1971.
12. C. P. Slichter, ''Principles of Magnetic Resonance'' (H. K. V. Lotsch, Ed.), 3rd ed., Chap. 2, Springer-Verlag, New York, 1990.
13. A. Abragam, ''The Principles of Nuclear Magnetism,'' Chap. 3, Clarendon Press, Oxford, 1961.
14. M. I. Dyakonov and V. I. Perel, *Sov. Phys.-JETP* **38,** 177 (1974).
15. V. L. Berkovits, A. I. Ekimov, and V. I. Safarov, *Sov. Phys.-JETP* **38,** 169 (1974).
16. D. Paget, *Phys. Rev. B* **24,** 3776 (1981).